Plant Pathol. J. 38(2) : 115-130 (2022)
https://doi.org/10.5423/PPJ.OA.01.2022.0004
pISSN 1598-2254 eISSN 2093-9280

Research Article Open Access

The Plant Pathology Journal

Identification, Characterization, and Efficacy Evaluation of *Bacillus velezensis* for Shot-Hole Disease Biocontrol in Flowering Cherry

Viet-Cuong Han[1], Nan Hee Yu[1], Hyeokjun Yoon[2], Neung-Ho Ahn[2], Youn Kyoung Son[2], Byoung-Hee Lee[2], and Jin-Cheol Kim[1]*

[1]*Department of Agricultural Chemistry, Institute of Environmentally-Friendly Agriculture, College of Agriculture and Life Science, Chonnam National University, Gwangju 61186, Korea*
[2]*Biological and Genetic Resources Assessment Division, National Institute of Biological Resources, Incheon 22689, Korea*

(Received on January 6, 2022; Revised on February 7, 2022; Accepted on February 8, 2022)

Though information exists regarding the pathogenesis of the shot-hole disease (SH) in flowering cherry (FC), there has been a lack of research focusing on SH management. Therefore, here, we investigated the inhibitory activities of antagonistic bacteria against SH pathogens both *in vitro* and *in vivo* as well as their biochemical characteristics and bioactive compounds. Two biosurfactant-producing bacterial antagonists, identified as *Bacillus velezensis* strains JCK-1618 and JCK-1696, exhibited the best effects against the growth of both bacterial and fungal SH pathogens *in vitro* through their cell-free culture filtrates (CFCFs). These two strains also strongly inhibited the growth of the pathogens via the action of their antimicrobial diffusible compounds and antimicrobial volatile organic compounds (VOCs). Crude enzymes, solvent extracts, and biosurfactants of the two strains exhibited antimicrobial activities. Liquid chromatography/electrospray ionization time-of-flight mass spectrometric analysis of the partially purified active fractions revealed that the two antagonists produced three cyclic lipopeptides, including iturin A, fengycin A, and surfactin, and a polyketide, oxydifficidin. In a detached leaf assay, pre-treatment and co-treatment of FC leaves with the CFCFs led to a large reduction in the severity of the leaf spots caused by *Epicoccum tobaicum* and *Bukholderia contaminans*, respectively. In addition, the two antagonists produced indole-3-acetic acid, siderophore, and a series of hydrolytic enzymes, along with the formation of a substantial biofilm. To our knowledge, this is the first report of the antimicrobial activities of the diffusible compounds and VOCs of *B. velezensis* against the SH pathogens and their efficiency in the biocontrol of SH.

Keywords **:** antagonistic bacteria, antimicrobial compounds, biological control, hydrolytic enzymes, volatile organic compounds

*Corresponding author.
Phone) +82-62-530-2132, FAX) +82-62-530-2139
E-mail) kjinc@jnu.ac.kr

Handling Editor : Youn-Sig Kwak

Flowering cherry (FC, *Prunus x yedoensis* Matsumura; Somei-yoshino) is an ornamental tree, planted across South Korea in parks or along roadsides and in forests, producing stunning flowers in the spring. Like all cherry trees, FC trees are susceptible to several diseases. The shot-hole disease (SH) is one of the most common and important diseases affecting FC trees every year, resulting in premature defoliation, decreased photosynthetic metabolism, reduced flowering of cherry blossoms in the following year, and increased susceptibility of trees to injuries during severe winters (Díaz et al., 2007; Gruber et al., 2012). Recently, we revealed several pathogens associated with SH in FC, including the bacteria *Bukholderia contaminans* (Bc), *Pseudomonas syringae* pv. *syringae* (Pss), and *Xanthomonas arboricola* pv. *pruni* (Xap) (Han et al., 2021a), and the fungi *Mycosphaerella cerasella* (Mc) and *Epicoccum tobaicum* (Et) (Han et al., 2021b).

In an attempt to protect plants, synthetic bactericides and fungicides have been routinely used to control plant microbial pathogens. However, the intensive use of synthetic agrochemicals has not only created problems of pathogen resistance to applied substances and increased soil contamination but may also have adverse high toxicity effects on human beings and microbial communities (Compant et al., 2005). Consequently, biological control has been suggested as an alternative strategy or a supplementary method for controlling plant diseases, perhaps as a part of an integrated management system, thus reducing the use of chemical products and contributing to environmental preservation (Compant et al., 2005).

Antagonistic bacteria have received much attention as biological control agents (BCAs) because of their beneficial effects and potential applications in the suppression of plant diseases through different modes of action. Bacterial antagonists can produce hydrolytic enzymes, antimicrobial substances, and volatile organic compounds (VOCs) that can suppress or kill phytopathogenic microbes (Senthilkumar et al., 2009). Further, the competition between the antagonistic bacteria and the disease-causing agents for the available nutrients and living spaces deters pathogen growth (Elad and Baker, 1985). Finally, bacterial antagonists are capable of forming biofilms, which contribute to both bacterial survival and host plant colonization, thus protecting plants from pathogens (Bais et al., 2004). In addition to acting as inhibitors against pathogens, antagonistic bacteria are likely to stimulate the growth of host plants, either by synthesizing hormones, such as indole-3-acetic acid (IAA) (Idris et al., 2007), or by promoting an increase in nutrient concentrations by phosphate solubilization and nitrogen fixation (Senthilkumar et al., 2009).

Among the most promising candidates for BCAs are several species of the genus *Bacillus*, such as *B. subtilis, B. velezensis,* and *B. licheniformis.* These species are regarded as safe microorganisms and possess several advantages that make them stand out from the members of other antagonistic bacterial genera. First, *Bacillus* spp. can produce endospores which are resistant to heat, UV light, and desiccation, which assure their prevalence in the environment and guarantee future suitable formulation strategies (Schallmey et al., 2004). Second, *Bacillus* spp. release a variety of active compounds with broad-spectrum antimicrobial activities (Cao et al., 2018; Chen et al., 2009; Xu et al., 2018).

Since the discovery of the pathogens causing SH in FC, there has been a lack of research focusing on SH management. Further, biological control using *Bacillus* antagonists has been proposed as a potential approach for disease control strategies since there are limitations to the use of synthetic bactericides and fungicides on FC trees grown on sidewalks, in parks and in forests. During the screening of 403 bacterial isolates, we found that two *Bacillus* strains, designated as JCK-1618 and JCK-1696, exhibited the strongest antimicrobial activity against the SH-causing pathogens. Here, we aimed to (1) identify the two bacterial strains JCK-1618 and JCK-1696 at the species level, (2) evaluate the inhibitory activities of the two bacterial strains against SH pathogens *in vitro* and *in vivo*, (3) assess the biochemical and phenotypic characteristics of the two bacterial strains that may be involved in antagonism and the stimulation of plant growth, and (4) elucidate both volatile and diffusible antimicrobial compounds produced by the two bacterial strains.

Materials and Methods

Plant pathogens. Xap P1, the causative agent of leaf spot on peach plants, and Mc, the leaf spot-causing agent of oriental cherry plants (*P. serrulata* var. *spontanea*), and the three pathogens inducing leaf spots and shot holes on FC (Et JCK-CSHF10, Bc JCK-CSHB12, and Pss JCK-CSHB44) (Han et al., 2021a, 2021b) were used. Mc and Et were cultured on potato dextrose agar/broth (PDA/PDB) (Becton, Dickinson, and Co., Heidelberg, Germany) (Becton, Dickinson, and Co., Heidelberg, Germany) at 25°C; Xap, Bc, and Pss were cultured on tryptic soy agar/broth (TSA/TSB) (Becton, Dickinson, and Co.) at 28°C.

Bacterial isolation. Soil samples for bacterial isolation were collected from soil at a depth of 5 to 10 cm from various crop and tree fields in South Korea. The bacteria were isolated by the plate dilution method. Soil suspension was spread onto sterilized and coagulated TSA plates. The bacterial isolates were purified and maintained on TSA plates at 4°C until further use.

To isolate bacterial endophytes from FC leaves, healthy and un-damaged leaf samples were collected at Chonnam National University (Gwangju campus, Gwangju, Korea). Approximately 3-mm-long sterilized leaf pieces were macerated into a suspension with 10 mM phosphate-buffered saline. Next, the suspension was spread over the surface of a TSA plate. Bacterial isolates were then picked and maintained following the aforementioned procedure. The methods were also described in detail in the Supplementary Methods.

Cell-free culture filtrate preparation. A single bacterial colony was cultured in 5-ml TSB in glass tubes for 48 h at 28°C under shaking conditions at 150 rpm/min. The cul-

ture broth was then centrifuged at 10,000 ×*g* at 4°C for 15 min. Next, the supernatant in the upper phase was collected before being passed through a 0.22-μm pore size filter unit (Minisart hydrophilic syringe filter; Goettingen, Germany) to obtain cell-free culture filtrate (CFCF), which was then used for antimicrobial activity testing and stored at –20°C until further use.

***In vitro* antimicrobial activity and minimum inhibitory concentration.** During the screening of 403 bacterial isolates (refer to the Supplementary Methods), we found that two isolates, designated as JCK-1618 and JCK-1696, exhibited the strongest antimicrobial activity against the SH-causing pathogens. The CFCFs of JCK-1618 and JCK-1696 were then determined for their minimum inhibitory concentration (MIC) against the pathogens. The microtiter broth dilution method was employed with 2-fold serial dilutions reaching a variety of CFCF concentrations (0.078% to 10%) (Nguyen et al., 2019). The lowest concentration of CFCFs which completely inhibited the growth of bacteria or fungi by visual observation was defined as the MIC value.

Molecular identification of bacteria. Two bacterial isolates (JCK-1618 and JCK-1696) were identified as described by Han et al. (2021a) with minor modifications. The conserved region of 16S rRNA (ribosomal ribonucleic acid) and *gryA* (DNA gyrase subunit A) genes were amplified with primers as follows: 9F/1512R (Faveri et al., 2008) and gryA-f/gryA-r (Chun and Bae, 2000), respectively. Multiple sequence alignments and the construction of a phylogenetic tree using concatenated sequences of 16S rRNA and *gryA* were performed using MEGA X (Kumar et al., 2018).

Incubation time optimization and bacterial growth curve construction. The optimum incubation periods for JCK-1618 and JCK-1696 at which the corresponding CFCFs exhibit the strongest antimicrobial activities were determined. The CFCFs obtained from an optimum time were devoted to an *in vivo* assay and the extraction of bioactive compounds. The methods were described in detail in the Supplementary Methods.

Dual-culture assay. JCK-1618 and JCK-1696 were tested for the quantification of the percentage inhibition of radius growth (PIRG) of Et using a dual-culture assay. A 5-mm plug of a 7-day-old pathogenic fungus culture grown on PDA was placed at the center of a new PDA plate (diameter 90 mm). Next, bacterial suspension, obtained from a 24-h culture, was streaked as a broad line, 2 cm away from the plug, on one side of the plate. The opposite side of the plate served as a control. After incubation at 25°C, the radius record of the colony growth of each fungus toward the bacteria-streaked side was established when the control side was fully covered with mycelia (radius 45 mm). The PIRG was then calculated using the formula PIRG = 100 × (C – T)/(C) (%), with C representing the radius of the mycelia on the side not having bacterial colonies (45 mm) and T representing the radius of mycelia toward the bacterial colonies (mm).

Spot-on-lawn assay. The antibacterial activities of JCK-1618 and JCK-1696 against bacterial pathogens were determined using an optimized spot-on-lawn assay (Cao et al., 2018).

Enzyme production. Extracellular hydrolytic enzyme activity was determined by the well-diffusion method for qualitative analysis. Wells were established in Petri plates with the enzyme induction medium to test the following enzymes: cellulase, chitinase, β-1,3-glucanase, chitosanase, amylase, and protease. Next, 40 μl of 48-h CFCFs, prepared as described above, or 40 μl TSB as negative controls were added into each well. After 72 h at 28°C, each plate was flooded with Lugol's iodine. The appearance of clear zones around the colonies confirmed enzyme production. The actual diameter of the clear zones caused by the enzymes was recorded in triplicate and calculated based on the formula V = (D – 5) (mm), with D representing the diameter of a clear zone and 5 representing well diameter (mm).

Secondary metabolite production. IAA production was determined using the methods described by Gordon and Weber (1951) with minor modifications. Bacteria were cultured in TSB supplemented with L-tryptophan (0.01, 0.05, and 0.1%). The amount of bacterial IAA was also quantified.

Siderophore and ammonia production were determined using methods described by Schwyn and Neilands (1987) and Xu and Kim (2014), respectively. Bacterial phosphate solubilization was determined as described by Nautiyal (1999).

Phenotypic characteristics. Swimming, swarming, and twitching motilities were determined as described by Tahir et al. (2017). A drop collapse assay of bacteria was performed as described by Kruijt et al. (2009).

Biofilm production was carried out on flat-bottom 96-

well plates (Gudiña et al., 2010; O'Toole et al., 1999). Two media, including TSB/TSA or TSBGM/TSAGM (TSB/TSA with 1% glycerol and 0.1 mM $MnSO_4$ added) (Shemesh and Chai, 2013), were used. Biofilm quantification was performed (Gudiña et al., 2010). Images of colony formation and pellicle formation were also photographed.

Preparation of crude enzyme. The 48-h CFCFs of JCK-1618 and JCK-1696 were used for the preparation of the crude enzyme following the methods described by Wang and Chang (1997) with minor modifications. A dialysis bag (10 kDa, Spectra/Por Dialysis Membrane, Fisher Scientific, Göteborg, Sweden) was employed for the dialysis process. The crude enzyme was sterilized before being examined for antimicrobial activity on 96-well plates as described above.

Antimicrobial test of bacterial VOCs

Antimicrobial activity of VOCs. Two-phase Petri plates were employed to test bacterial VOCs against pathogens. First, TSA was administered to one compartment of the plate, followed by antagonistic bacteria being streaked over the surface one day and three days before culturing the test pathogens. For antifungal activity test, a 7-day-old fungal plug (Mc or Et) was placed in the remaining compartment containing PDA. For antibacterial activity test, 10 µl of Xap suspension (10^7 cfu/ml) was spot-inoculated in three sites in the remaining compartment containing TSA. Plates containing only bacterial and fungal pathogens served as negative controls. Inoculated plates were sealed with Parafilm. Some inoculated plates were not sealed with Parafilm to assess the normal growth of pathogens. Plates containing pathogenic fungi and bacteria were incubated at 25°C and 30°C, respectively. Fungal growth was evaluated in terms of the diameter of the mycelial growth while bacterial pathogens were evaluated in terms of both colony diameter (mm) and bacterial population (measured at OD_{600}). The percentage inhibition of bacterial and fungal growth was then calculated (%).

Collection of volatile compounds. Each bacterial strain was inoculated into 20 ml of TSA in a 100-ml vial with a solid phase micro-extraction fiber inserted into the headspace. Vials containing only TSA served as negative controls. The inoculated vials were then incubated at 30°C for 72 h. The volatile trap was then inserted into the vials to absorb VOCs while the vials were maintained at 60°C for 35 min on a hot plate.

VOC analysis by gas chromatography-mass spectrometry. VOCs released by JCK-1618 and JCK-1696 were analyzed by gas chromatography-mass spectrometry (GC-MS; Shimadzu GC-MS QP5050, Shimadzu Co., Kyoto, Japan). The volatile trap containing VOCs was injected into the injection port of the GC-MS. Each run was performed for 41 min in the split-less injection mode. The cycle was initialized at 30°C for 2 min and then increased to 250°C at 10°C per min. The carrier gas (helium) was administered at a flow rate of 3 ml per min. The mass spectra of unknown VOCs were compared to those submitted in the NIST/EPA/NIH Mass Spec. Library (version 2.0). The quantities of VOCs were expressed as relative area concentrations and corrected by taking into consideration the area of the compounds detected in the negative controls.

Detached leaf assay. The disease control efficacy of the CFCFs of JCK-1618 and JCK-1696 at 5-, 10-, 20-, and 50-fold dilutions were evaluated against the development of FC leaf spots using a detached leaf assay. Daisen M45 (mancozeb 75%; FarmHannong Co., Ltd., Seoul, Korea) and Sungbocycline (oxytetracycline 17%; Sungbo Chemicals Co., Ltd., Seoul, Korea) were used as positive controls for fungus- and bacterium-induced leaf spots on FC, respectively. All the above-mentioned formulas were diluted using sterile distilled water (SDW). SDW and TSB were also applied as negative controls. For the biocontrol of leaf spot symptoms caused by Et, the leaf surface was pre-treated with 8 µl of the formulas for 24 h before the inoculation of the fungal mycelial plugs (5 mm) (Zlatković et al., 2016), while for the biocontrol of symptoms induced by Bc, leaves were infiltrated with pathogenic bacterial suspension (Hulin et al., 2018) and subsequently treated with 5 µl of the formulas. This work was carried out on three leaves per treatment, with three inoculation sites per leaf, totaling nine inoculation sites in each treatment for fungal inoculation, and eight inoculation sites on each leaf leading to 24 inoculation sites for bacterial inoculation. Treated leaves were then placed in 150-mm Petri plates containing water agar (0.8% agar) and incubated for 7 to 10 days at 24°C and 28°C for fungal and bacterial inoculation, respectively. Disease symptoms were scored from 0 to 5 as described by Hulin et al. (2018). Disease symptom severity value (DS) was measured before calculating the reduction of disease symptoms (%) as described by Lee at al. (2006) with minor modifications. DS was calculated using the formula DS (%) = ((∑ (the number of diseased inoculation sites × disease severity score))/(5 × the number of inoculation sites rated)) × 100.

Biosurfactant production and isolation. Biosurfactants

were obtained from bacterial cells before being lyophilized according to the methods described by De Souza et al. (2003) and Gudiña et al. (2010).

Extraction of crude extracts. A 400-ml aliquot of the culture supernatant of each strain (JCK-1618 and JCK-1696) was extracted twice successively with ethyl acetate (EA) and *n*-butanol (BuOH). The organic layers were dried into concentrates to obtain the crude extracts. The crude extracts were then dissolved in methanol (MeOH) before being tested for antimicrobial activity ranging from 500 to 1.95 µg/ml against the pathogens using the microtiter broth dilution method.

Determination of agar-diffusible antimicrobial metabolites

Separation of active metabolites. Both EA and BuOH extracts of JCK-1618 and JCK-1696 showed *in vitro* antibacterial and antifungal activities against the test pathogens. To locate the positions of the active metabolites on the thin-layer chromatography (TLC) plates, bioautography was conducted. The extracts were loaded onto TLC plates before being developed using a solvent system of chloroform:methanol:water (14:6:1, v/v/v). The developed TLC plates were submerged in TSA supplemented with Xap suspension (10^5 cfu/ml) or PDA amended with the fungal mycelial suspension of Et (0.5 mg/ml) in Petri dishes. After 3 days, spots on TLC plates displaying clear inhibitory zones were noted and used as a standard for the further purification process.

TLC analysis revealed that the two strains produced almost identical active metabolites (Supplementary Fig. 1). Based on the observations, these two strains were confirmed as possessing a similar profile of active compounds. Therefore, only JCK-1618 was selected for agar-diffusible active metabolite isolation. EA and BuOH extracts from JCK-1618 were loaded separately onto preparative TLC plates (0.5-mm layer thickness), followed by developing in the aforementioned solvent system. Further, five fractions, including three fractions from the EA extract and two fractions from the BuOH extract, showed antimicrobial activities. The five fractions were pooled and then loaded into a Sephadex LH-20 column (diameter: 1 cm; length: 40 cm) with MeOH serving as a diluent. Two active fractions (F4 and F5) were found to inhibit the growth of Mc, Et, and Xap, with F4 exhibiting a stronger antimicrobial activity than F5. Next, F4 was loaded on TLC for further detection of active compounds. Spots revealing the location of three cyclic lipopeptides (iturin A, surfactin, and fengycin A; Merck KgaA, Darmstadt, Germany) and two polyketides (difficidin and oxydifficidin) (Im et al., 2020) were detected by comparing them to those of the respective purified compounds representing antimicrobial compounds produced by the genus *Bacillus*. Further, F4 was analyzed using liquid chromatography/electrospray ionization time-of-flight mass spectrometry (LC-ESI-TOF-MS) to detect antimicrobial compounds.

LC-ESI-TOF-MS. The active fraction F4 was subjected to electrospray ionization-mass spectrometry using a hybrid quadrupole-TOF mass spectrometry system (QSTAR XL; AB Sciex Instruments, San Diego, CA, USA) to identify its active compounds. All mass spectrometric analyses were performed by positive/negative electrospray ionization (ESI+/ESI–) with Ultra Performance Liquid Chromatography using a C18 reversed-phase column (Acquity UPLC BEH C18, 1.7 µm particle size, 2.1 × 100 mm; Waters, MA, USA). Active compounds were eluted by two solvent systems, including solvent A (0.1% formic acid in water) and solvent B (0.1% formic acid in acetonitrile). The flow rate for the two elution programs was 300 µl/min, and the column temperature was maintained at 40°C. A 5-µl aliquot was injected into the system and the gradient program was conducted as follows: 0-1 min and 16-20 min, 95% A and 5% B; 10-15 min, 100% B. Liquid chromatography mass spectrometry full-scan spectra were acquired.

Statistical analysis. All experiments were repeated in triplicate. Statistical analyses and boxplot generation were performed in R 3.5.2 (R Core Team, 2018) with the packages 'multcompView' and 'ggplot2', respectively. Normal data distribution and variance homogeneity were checked using the Shapiro-Wilk and Kruskal-Wallis tests. Significant differences ($P < 0.05$) between treatments were analyzed by one-way analysis of variance (ANOVA), followed by Tukey's honestly significant difference test.

Results

Isolation and screening of antagonistic bacteria. Of the 403 bacterial strains isolated, two strains, designated as JCK-1618 (obtained from the soil in Jeju island) and JCK-1696 (an endophyte purified from healthy FC leaves), exhibited the best effects against the growth of the pathogens. Therefore, these strains were selected for further experiments.

Identification of JCK-1618 and JCK-1696. Blast analysis indicated that the 16S rRNA sequences of JCK-1618 and JCK-1696 (accession numbers MW193331 and

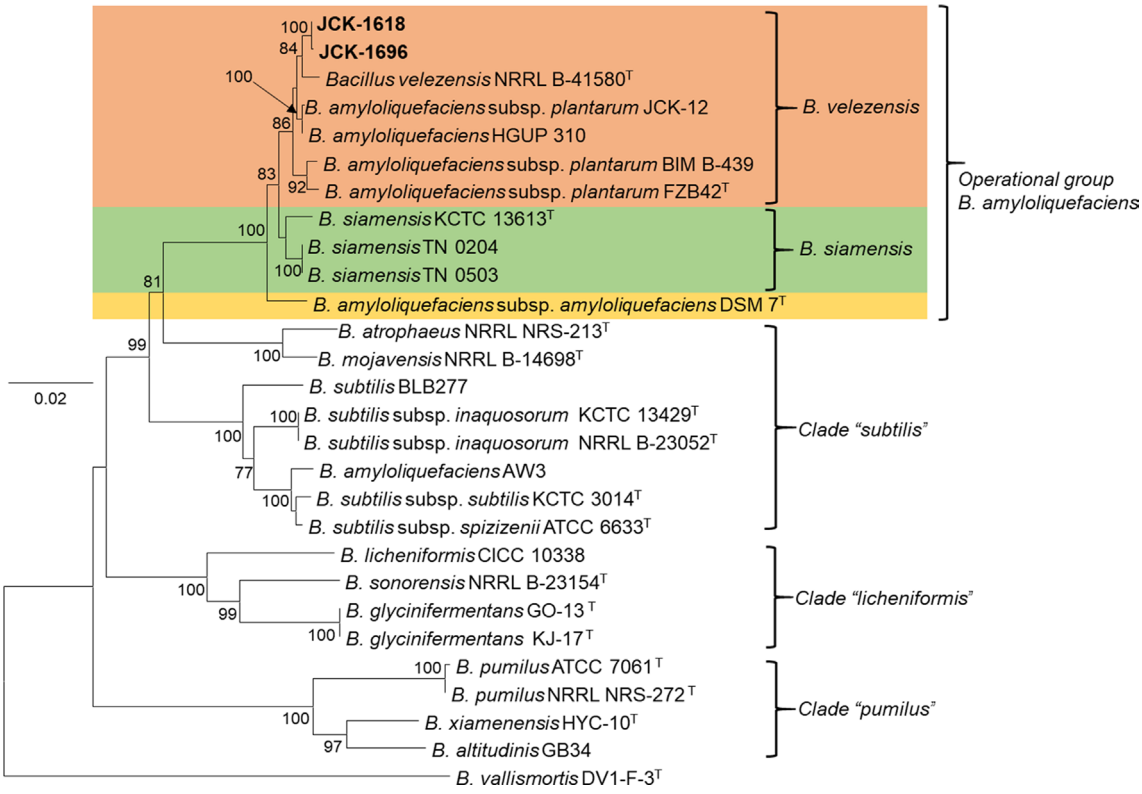

Fig. 1. Neighbor-joining phylogenetic tree based on Kimura 2-parameter + G model using the concatenated nucleotide sequences of 16S rRNA and *gyrA* of 26 strains representing the species in the genus *Bacillus.* Bootstrap support values above 70% (from 1,000 replicates) are given at the nodes. The scale bar represents substitution sites. The tree is rooted to *Bacillus vallismortis* (DV1-F-3).

MW193332, respectively) shared 100% identity with a variety of strains of *B. amyloliquefaciens* and *B. velezensis.*

Since 16S rRNA was not sufficient to differentiate between the *Bacillus* species, we employed the *gyrA* gene to assist in identification. BLAST analysis indicated that the *gyrA* gene sequences of JCK-1618 and JCK-1696 (MW419811 and MW419812, respectively) shared high identity with the sequences of other *B. velezensis* strains deposited in GenBank, including NAU B55 (FN652788, 100%), 41B-1 (KF601552, 99.7%), and NRRL BD-545 (EU138626, 99.6%).

The construction of the phylogenetic tree, using the concatenated nucleotide sequences of 16S rRNA and *gyrA,* showed that JCK-1618 and JCK-1696 were identical to each other. Additionally, JCK-1618 and JCK-1696 formed a cluster with the *B. velezensis* type strain NRRL B-41580 within the clade of *B. velezensis*, belonging to an operational group *B. amyloliquefaciens*, which contained *B. velezensis* (prior synonym for *B. methylotrophicus*, *B. amyloliquefaciens* subsp. *plantarum*, and *B. oryzicola*) (Dunlap et al., 2016), *B. siamensis,* and *B. amyloliquefaciens* subsp. *amyloliquefaciens* (Fan et al., 2017) (Fig. 1). Thus, both JCK-1618 and JCK-1696 were identified as *B. velezensis.*

Incubation time optimization and growth curve construction. The results showed that the CFCFs obtained from the 48 h-incubated broth culture exhibited the best effects against the growth of Mc, Et, and Xap (MICs = 1.25, 1.25, and 0.3125%, respectively) (Table 1, Supplementary Table 1, Supplementary Fig. 2A), indicating that 48 h is an optimum incubation time for JCK-1618 and JCK-1696. Further, the 48-h CFCF of JCK-1618 and JCK-1696 exhibited MICs at 2.5 and 5% against Bc and Pss, respectively (Supplementary Fig. 2A). Additionally, growth curves of JCK-1618 and JCK-1696 were constructed (Supplementary Fig. 3). It was noted that both strains experienced an autolysis stage.

Inhibition of pathogen growth by agar-diffusible compounds of JCK-1618 and JCK-1696. Both JCK-1618 and JCK-1696 inhibited the growth of the fungal and bacterial pathogens tested by the diffusible antimicrobial substances released in the solid media (Table 1, Supplementary Fig. 2B and C). JCK-1618 and JCK-1696 caused the mycelial growth inhibition of Et with efficacies of 80.7 and 81.5%,

Table 1. Growth inhibition of flowering cherry shot-hole pathogens caused by JCK-1618 and JCK-1696 in microtiter broth dilution, dual-culture, and spot-on-lawn assays

Strain	MIC (% CFCF)					Growth inhibition (%)		Inhibition zone (mm)		
	Mc	Et	Xap	Bc	Pss	Mc	Et	Xap	Bc	Pss
JCK-1618	1.25	1.25	0.3125	2.5	5	NT	80.7 a	20.5 ± 0.5 a	15.7 ± 0.6 a	15.5 ± 0.5 a
JCK-1696	1.25	1.25	0.3125	2.5	5	NT	81.5 a	20.3 ± 0.6 a	15.8 ± 0.8 a	15.8 ± 0.3 a

The values represent the average of data recorded in triplicate; the values in the same column followed by a similar letter(s) indicate no significant differences in the analysis (Tukey's HSD test, $P < 0.05$).
MIC, minimum inhibitory concentration; CFCF, cell-free culture filtrate; Mc, *Mycosphaerella cerasella*; Et, *Epicoccum tobaicum*; Xap, *Xanthomonas arboricola* pv. *pruni*; Bc, *Bukholderia contaminans*; Pss, *Pseudomonas syringae* pv. *syringae*; NT, not tested; HSD, honestly significant difference.

Table 2. Growth inhibition of flowering cherry shot-hole-causing pathogens by antimicrobial VOCs produced by JCK-1618 and JCK-1696

Strain	Inoculation time	Percentage of growth inhibition (%)			
		Mc	Et	Xap	
				Colony diameter	Cell multiplication
JCK-1618	1 dbi	56.3 c	39.0 b	22.4 b	51.4 d
	3 dbi	74.8 a	61.0 a	36.2 a	60.3 b
JCK-1696	1 dbi	67.0 b	44.9 b	23.2 b	54.3 c
	3 dbi	75.7 a	66.8 a	39.8 a	72.2 a

Numbers in the same column followed by a different letter(s) indicate significant variations in the analysis (Tukey's HSD test, $P < 0.05$).
VOC, volatile organic compound; Mc, *Mycosphaerella cerasella*; Et, *Epicoccum tobaicum*; Xap, *Xanthomonas arboricola* pv. *pruni*; dbi, days before pathogen inoculation; HSD, honestly significant difference.

respectively. These values were not significantly different from each other. This trend was also observed with the inhibition zone diameters of Xap, Bc, and Pss caused by JCK-1618 and JCK-1696. Indeed, Xap was found to be most sensitive to the two bacterial antagonists with inhibition zones of over 20 mm, followed by Bc and Pss. The antifungal activity of the two antagonists against the fungus Mc on solid media was not assessed because Mc grew very slowly.

Inhibition of pathogen growth by the VOCs of JCK-1618 and JCK-1696. In addition to the inhibition of pathogens by antimicrobial diffusible compounds, JCK-1618 and JCK-1696 produced VOCs interfering with the growth of Mc, Et, and Xap (Supplementary Fig. 4). The inhibition efficacy against the two fungi, Mc and Et, ranged from 39 to 75.7%, while the percentage of growth inhibition against Xap ranged from 22.4% to 72.2% (Table 2). Notably, the two antagonists that were inoculated on the media for 3 days before pathogen inoculation (dbi) exhibited significantly stronger antimicrobial activity than those being inoculated for one dpi.

GC-MS analysis of detected VOCs. The VOC profiles of JCK-1618 and JCK-1696 exhibited many similarities (Supplementary Tables 2-4, Supplementary Fig. 5). In particular, 3-methyl-1-butanol, 2-nonanone, 2-decanone, and 2-undecanone were found to be the most abundant in both strains. Additionally, almost all identified VOCs were previously confirmed as antimicrobial substances. While 2-undecanone (Raza et al., 2016) and 2-tridecanone (López-Lara et al., 2018) have been reported as antibacterial substances, 3-methyl-1-butanol (Chaves-López et al., 2015), dimethyl disulfide (Li et al., 2010), toluene (Yuan et al., 2012), 5-methyl-2-heptanone (Morita et al., 2019), 2-decanone (Fernando et al., 2005; Yuan et al., 2012; Zheng et al., 2013), 2-dodecanone (Yuan et al., 2012), and 1-hexadecene (Zhang et al., 2013) have previously been confirmed as antifungal metabolites. Interestingly, 2-nonanone has been reported to inhibit the growth of both pathogenic bacteria and fungi (Fernando et al., 2005; Raza et al., 2016; Yuan et al., 2012; Zheng et al., 2013).

Disease control efficacy of JCK-1618 and JCK-1696 against SH in a detached leaf assay. Treatment of the 48-h CFCFs of JCK-1618 and JCK-1696 resulted in a great reduction in the disease severity of Et infection (Fig. 2). Five-fold-diluted CFCFs of both strains reduced symptom

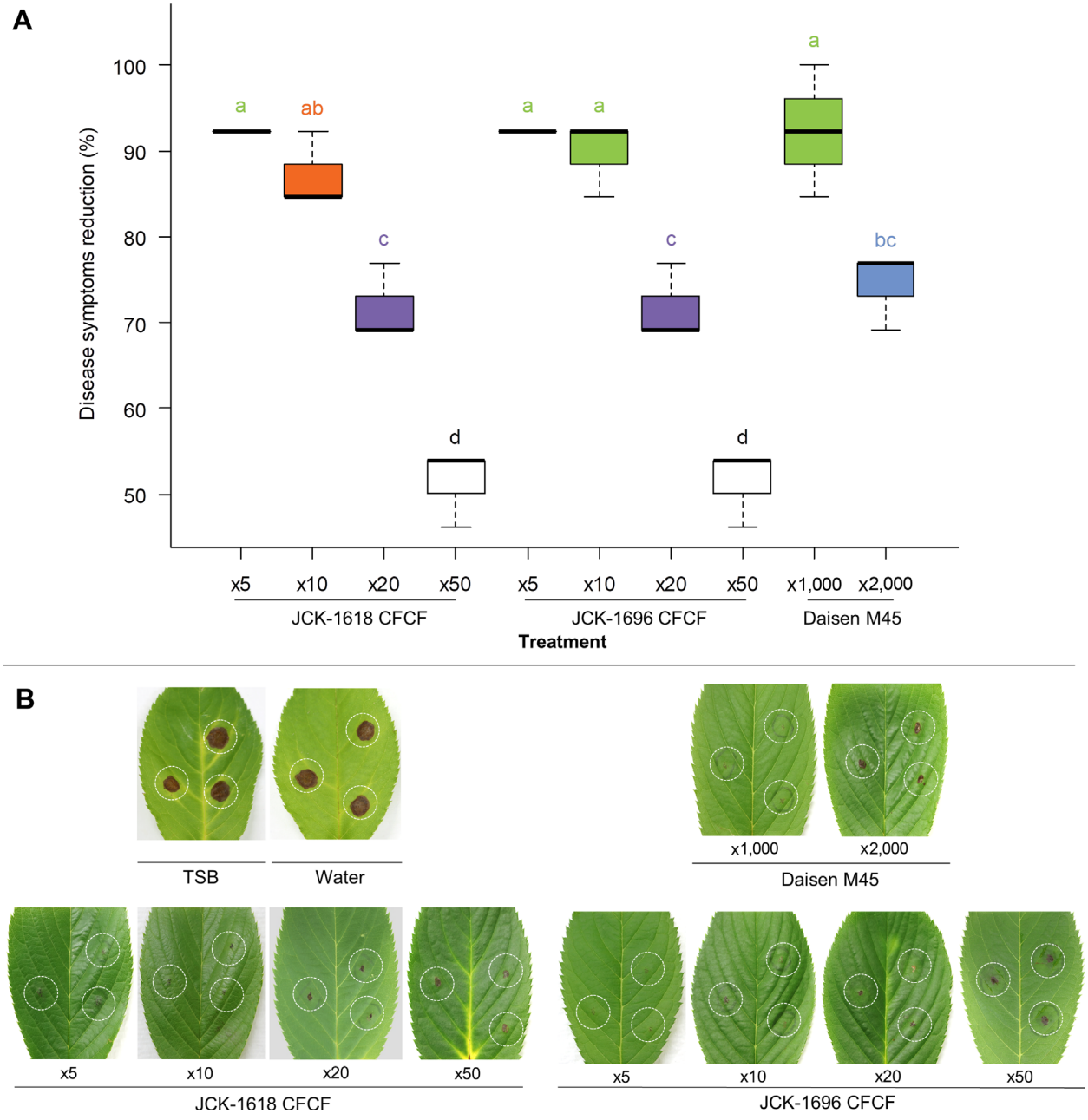

Fig. 2. JCK-1618 and JCK-1696 suppressing brown spot symptoms of flowering cherry leaves caused by *Epicoccum tobaicum* in a detached leaf assay. The leaf surface was pre-treated with 8 µl of the formulas for 24 h before the inoculation of the fungal mycelial plugs. ×5, ×10, ×20, and ×50 represent 5-, 10-, 20-, and 50-fold dilutions, respectively. (A) Disease control efficiency. (B) Disease symptom development suppressed. Box plots with the same letter(s) indicate no significant differences in the analysis (Tukey's HSD test, $P < 0.05$). CFCF, cell-free culture filtrate; TSB, tryptic soy broth; HSD, honestly significant difference.

severity by 92.3%, similar to that observed with Daisen M45 (a.i. mancozeb) applied at 1,000-fold dilution. Notably, there was no significant variation between the attenuation of symptoms caused by 5-fold CFCF dilutions and 10-fold CFCF dilutions.

Treatment of 48-h CFCFs of JCK-1618 and JCK-1696 also strongly reduced disease severity of Bc infection in a dose-dependent manner (Fig. 3). The application of the 5-fold CFCF dilution showed an over 82% decrease in the severity of symptoms, similar to the result of the 1,000-fold dilution of Sungbocycline (a.i. oxytetracycline). Additionally, 10-fold and 50-fold CFCF dilutions led to disease

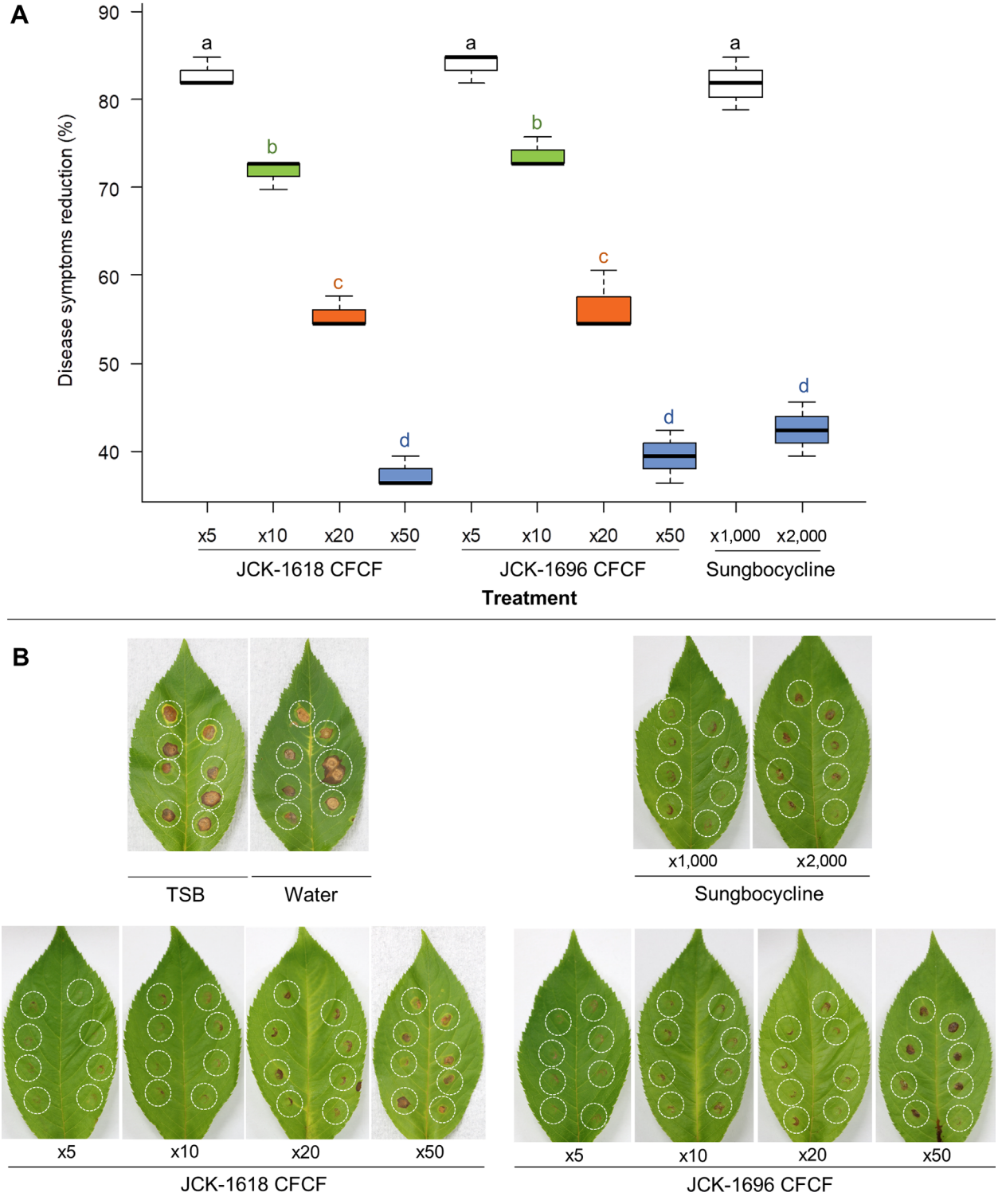

Fig. 3. JCK-1618 and JCK-1696 suppressing brown spot symptoms of flowering cherry leaves caused by *Bukholderia contaminans* in a detached leaf assay. Leaves were infiltrated with pathogenic bacterial suspension and subsequently treated with 5 µl of the formulas. ×5, ×10, ×20, and ×50 represent 5-, 10-, 20-, and 50-fold dilutions, respectively. (A) Disease control efficiency. (B) Disease symptom development suppressed. Box plots with the same letter(s) indicate no significant differences in the analysis (Tukey's HSD test, $P < 0.05$). CFCF, cell-free culture filtrate; TSB, tryptic soy broth; HSD, honestly significant difference.

Table 3. Biochemical and phenotypic characteristics of JCK-1618 and JCK-1696

Characteristic	Strains		Characteristic	Strains	
	JCK-1618	JCK-1696		JCK-1618	JCK-1696
Motility	+	+	Drop collapse assay	+	+
Protease	33.5 ± 0.5 a	33.8 ± 1.0 a	Biofilm	+	+
Chitinase	40.0 ± 1.0 a	40.2 ± 0.8 a	IAA	+	+
Cellulase	33.7 ± 1.2 a	33.5 ± 0.9 a	P solubilization	–	–
β-1,3-glucanase	39.0 ± 1.0 a	39.2 ± 0.8 a	Siderophore	+	+
Chitosanase	33 ± 1.0 a	33.3 ± 0.6 a	TSB growth	Orange	White
Amylase	25.7 ± 0.3 a	21.5 ± 0.5 b	Ammonia	+	+

Numbers indicate the mean diameter (mm) of the clear zones caused by an enzyme in triplicate ± standard deviation (n = 3). Numbers in the same row followed by a different letter (s) indicate significant variation in the analysis (Tukey's HSD test, $P < 0.05$).
+, positive; –, negative; IAA, indole-3-acetic acid; TSB, tryptic soy broth; HSD, honestly significant difference.

severity reductions of over 71% and 37%, respectively.

Biochemical and phenotypic characteristics. The biochemical and phenotypic results of JCK-1618 and JCK-1696 were shown in Table 3 and Supplementary Fig. 6. The two strains produced a variety of hydrolytic enzymes, including amylase, cellulase, chitosanase, chitinase, protease, and β-1,3-glucanase. Results from the qualitative analysis of these enzymes based on the clear zone diameters (CZDs) showed that the two antagonists secreted the same levels of all enzymes tested, of which the levels of chitinase were the highest (CZD > 40 mm), followed by those of β-1,3-glucanase (CZD ~39 mm), chitosanase, cellulase, and protease (CZDs ~33 mm) ($P < 0.05$). In addition, JCK-1618 and JCK-1696 released secondary metabolites, such as siderophore, ammonia, and IAA. The highest levels of IAA (17.26 and 16.2 µg/ml for JCK-1618 and JCK-1696, respectively) were recorded for the media supplemented with 0.1% L-tryptophan, followed by the media supplemented with 0.05% and 0.01% L-tryptophan. In contrast, both strains were negative for P solubilization.

Phenotypic characteristics of JCK-1618 and JCK-1696 revealed positive drop collapse assay results, indicating that both strains produced biosurfactants (Supplementary Fig. 6G). Both strains were also capable of swimming, swarming, and twitching (Supplementary Fig. 6A). Additionally, JCK-1618 and JCK-1696 both formed substantial biofilms, of which the biofilm formation obtained from the TSBGM or TSAGM medium was stimulated when compared to that obtained from TSB or TSA (Supplementary Fig. 6D-F). While JCK-1618 resulted in reddish-orange colonies when grown in TSB, JCK-1696 resulted in white colonies (Supplementary Fig. 6I).

Antimicrobial activity of crude enzymes, biosurfactants, and solvent extracts. Crude enzymes and biosurfactants obtained from JCK-1618 and JCK-1696 displayed antimicrobial activities against the pathogens tested (Table 4). Crude enzymes exhibited MICs ranging from 2.5 to 5% against Mc, Et, and Xap, while MICs for Bc and Pss

Table 4. MICs of the crude enzymes, crude biosurfactants, crude solvent extracts, and active fractions against FC shot-hole pathogens

Strain	MIC (µg/ml or %)				
	Mc	Et	Xap	Bc	Pss
JCK-1618					
Crude enzyme	5	5	5	>10	>10
Biosurfactant	250	250	31.25	250	250
EtOAc extract	250	125	15.6	125	125
BuOH extract	125	62.5	15.6	250	250
JCK-1696					
Crude enzyme	5	5	2.5	>10	>10
Biosurfactant	250	500	31.25	250	250
EtOAc extract	250	250	15.6	125	125
BuOH extract	125	125	15.6	250	250
F4	50	50	6.25	50	50
F5	100	100	12.5	100	>100
Oxolinic acid	NT	NT	0.39	0.625	0.625
Oxytetracycline	NT	NT	1.56	25	0.078
Streptomycin sulfate	NT	NT	12.5	>100	0.78
Difenoconazole	0.024	1.56	NT	NT	NT

MIC, minimum inhibitory concentrations; FC, flowering cherry; Mc, *Mycosphaerella cerasella*; Et, *Epicoccum tobaicum*; Xap, *Xanthomonas arboricola* pv. *pruni*; Bc, *Bukholderia contaminans*; Pss, *Pseudomonas syringae* pv. *syringae*; F4, F5, partially purified active fractions; NT, not tested.

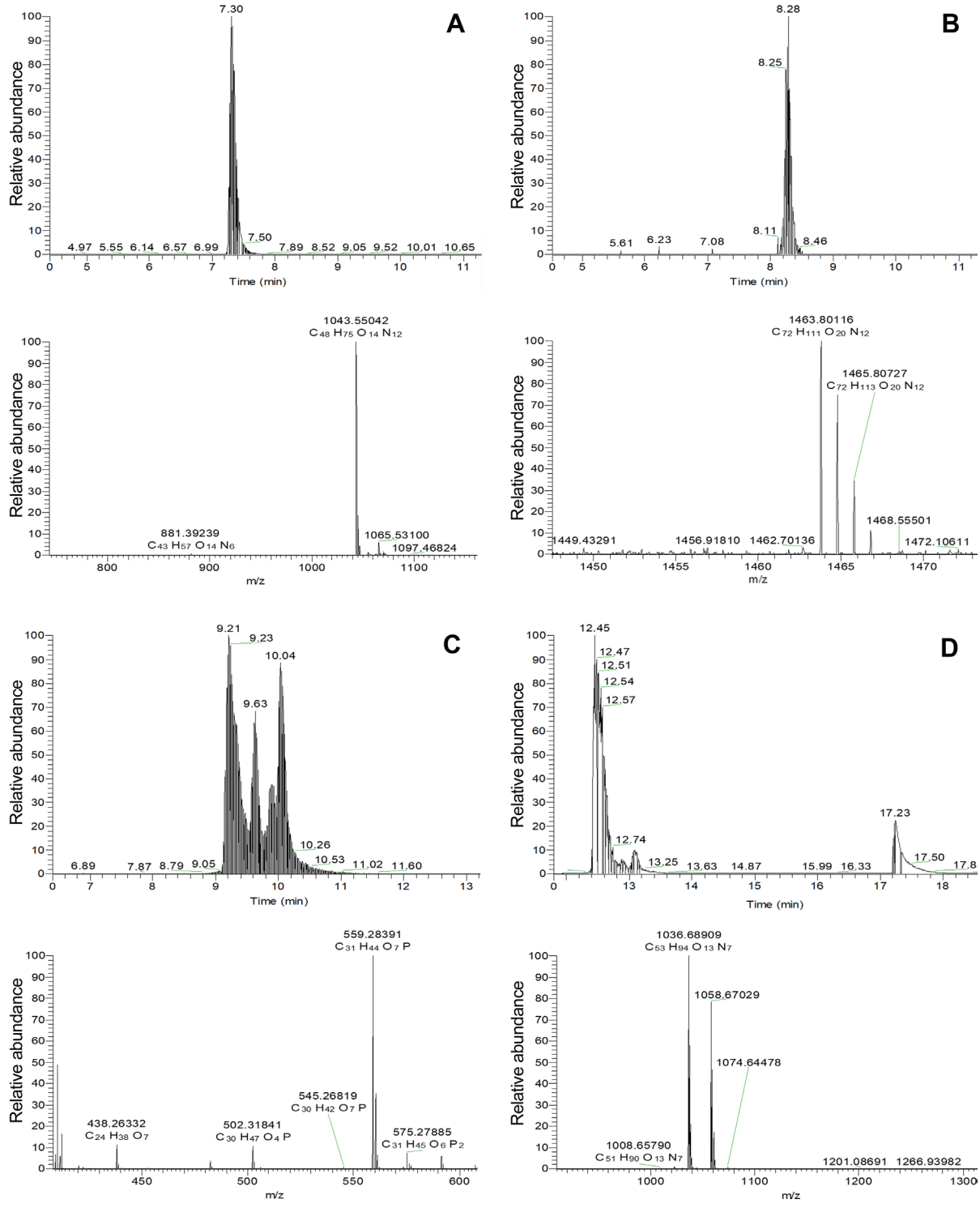

Fig. 4. LC-TOF-ESI-MS analysis of the bioactive compounds from the partially purified active fraction F4. (A) C_{14} Iturin A ($[M+H]^+$, *m/z* = 1,043.55042; $[M+Na]^+$, *m/z* = 1,065.53100). (B) C_{16} Fengycin A ($[M+H]^+$, *m/z* = 1,463.80116 and its isotopic peak at *m/z* 1465.80727). (C) Oxydifficidin ($[M-H]^-$, *m/z* = 559.28391). (D) C_{15} Surfactin ($[M+H]^+$, *m/z* = 1036.68909; $[M+Na]^+$, *m/z* = 1,058.67029). LC-TOF-ESI-MS, liquid chromatography/electrospray ionization time-of-flight mass spectrometry.

were higher than 10%. Biosurfactants inhibited the growth of Mc, Et, Bc, and Pss with MICs from 250 to 500 µg/ml. Notably, Xap was found to be the most sensitive to biosurfactants (MIC = 31.25 µg/ml).

Table 5. Summary of bioactive compounds detected from the partially purified active fraction F4 by LC-ESI-MS analysis

RT (min)	*m/z* $[M+H]^+$	*m/z* $[M-H]^-$	*m/z* $[M+Na]^+$	Identification	Reference
9.02-9.46	ND	559.28	ND	Oxydifficidin	Wilson et al. (1987),
9.50-9.68	ND	559.28	ND		Im et al. (2020)
9.78-9.93	ND	559.28	ND		
9.94-10.16	ND	559.28	ND		
6.50-6.72	1,015.52	1,013.51	1,037.50	C_{12} Iturin A	Xu et al. (2018)
6.76-7.06	1,029.54	1,027.52	1,051.52	C_{13} Iturin A	
7.14-7.49	1,043.55	1,041.54	1,065.53	C_{14} Iturin A	
7.43-7.81	1,057.57	1,055.55	1,079.55	C_{15} Iturin A	
7.84-8.19	1,071.58	1,069.57	1,093.56	C_{16} Iturin A	
8.15-8.42	1,085.60	1,083.58	1,107.58	C_{17} Iturin A	
8.22-8.38	1,463.80	ND	ND	C_{16} Fengycin A	Bie et al. (2009),
8.22-8.38	1,477.81	ND	ND	C_{17} Fengycin A	Xu et al. (2018)
11.43-11.55	994.64	992.63	ND	C_{12} Surfactin	Xu et al. (2018)
11.60-11.92	1,008.66	1,006.64	ND	C_{13} Surfactin	
12.03-12.25	1,022.67	1,020.66	1,044.67	C_{14} Surfactin	
12.38-12.59	1,036.68	1,034.67	1,058.67	C_{15} Surfactin	
17.24	1,036.69	ND	1,058.67	C_{15} Surfactin	

LC-ESI-MS, liquid chromatography/electrospray ionization mass spectrometry; RT, retention time; ND, not detected.

In addition, crude extracts (BuOH and EA layers) obtained from the two strains exhibited antimicrobial activities against all the pathogens tested, of which Xap remained the most susceptible (MIC = 15.6 µg/ml). The MICs of crude solvent extracts against the remaining pathogens varied from 62.5 to 250 µg/ml (Table 4).

Identification of antimicrobial metabolites isolated from crude solvent extracts. Two active fractions, designated as F4 and F5, were partially purified from the crude solvent extracts. Both showed antimicrobial activity against the pathogenic fungi and bacteria tested. MICs of F4 for Mc, Et, Xap, Bc, and Pss were 50, 50, 6.25, 50, and 50 µg/ml, respectively (Table 4).

TLC and high-performance liquid chromatography analyses of F4 indicated the presence of iturin A, surfactin, fengycin A, and oxydifficidin (data not shown). To further confirm the existence of these compounds, F4 was analyzed by LC-ESI-TOF-MS. The results displayed a $[M-H]^-$ ion peak at *m/z* 559.28, giving an identical molecular formula of $C_{31}H_{44}O_7P$ to oxydifficidin, as previously reported in the literature (Table 5, Fig. 4C). Additionally, $[M+H]^+$ ion peaks appeared at *m/z* 1,043.55, 1,057.57, 1,071.58, and 1,085.60 *m/z* (different to 14 Da, suggesting a difference in the presence of a –CH2 in the side chain), representing homologues of iturin A with C_{12} to C_{17} β-OH fatty acids, whose structures were confirmed by the presence of a complementary sodium adduct molecular ion $[M+Na]^+$ at *m/z* 1,037.50, 1,051.52, 1,065.53, 1,079.55, 1,093.56, and 1,107.58, respectively (Table 5, Fig. 4A). The $[M+H]^+$ ion peak at *m/z* 1,463.8 (isotopic peak at *m/z* 1,465.8), giving the molecular formula of $C_{72}H_{111}O_{20}N_{12}$ and *m/z* 1,477.81, represented a mass spectrometric signature for C_{16} and C_{17} fengycin A (Table 5, Fig. 4B). Four known cyclic surfactins, with acyl chain lengths ranging from C_{12} to C_{15}, were also detected based on the protonated ion $[M+H]^+$ at *m/z* 994.64, 1,008.66, 1,022.67, and 1,036.68 (and 1,036.69), respectively, while sodium adducts *m/z* 1,044.67 and 1,058.67 were assigned as 14- and 15-C β-OH fatty acids (Table 5, Fig. 4D). Taken together, three cyclic lipopeptides (CLPs), including iturin A, fengycin A, and surfactin, and a polyketide, oxydifficidin, were detected in F4, suggesting that these compounds were the main antimicrobial agents of JCK-1618 and JCK-1696. The chemical structures of the above-mentioned compounds were shown in Supplementary Fig. 7.

Discussion

Since the discovery of the pathogens causing SH in FC, there has been no research focusing on SH management. In this study, we applied a new approach, using *Bacillus* antagonists, for the biocontrol of SH because of the limitations of using synthetic pesticides on FC trees grown in public areas and in forests. Therefore, to our knowledge, our study is the first to fill the knowledge gap regarding the

management of SH in FC.

In this study, the two *B. velezensis* strains JCK-1618 and JCK-1696 strongly inhibited the mycelial growth of Mc, Et, and other pathogenic fungi and oomycetes (data not shown) through diffusible antifungal substances, thus indicating that JCK-1618 and JCK-1696 display a broad spectrum of antifungal activity. This is in line with the reports of *B. amyloliquefaciens* JCK-12 (Kim et al., 2017) and *B. simensis* JFL15 (Xu et al., 2018). The antibacterial activity of *B. velezensis* has also been reported (Im et al., 2020; Wu et al., 2015). In the present study, the two *B. velezensis* strains strongly suppressed the growth of bacterial pathogens causing SH on FC, further confirming their application as antibacterial biocontrol agents.

Bacillus antagonists are well-known for harboring various mechanisms to inhibit the growth of pathogenic microbes. Indeed, JCK-1618 and JCK-1696 emitted VOCs, interfering with the growth of bacterial and fungal pathogens. Some of the VOCs secreted by JCK-1618 and JCK-1696 have also been detected as antimicrobial compounds, including 2-nonanone, 3-methyl-1-butanol, 2-undecanone, 2-decanone, 2-dodecanone, and 5-methyl-2-heptanone. Therefore, it is proposed that these volatile compounds play a key role in the inhibitory activity of JCK-1618 and JCK-1696 toward the pathogens tested.

Several studies have attempted to determine the effectiveness of fungicides on controlling cherry leaf spots, primarily incited by the fungi Mc and *Blumeriella jaapii*. Proffer et al. (2013) reported that treatments with dodine or fluopyram were among the most effective for controlling cherry leaf spots on sour cherry (*P. cerasus*). Williams-Woodward (1998) demonstrated that mancozeb significantly reduce the severity of leaf spots on cherry laurel (*P. laurocerasus*). Similarly, in a detached leaf assay, this study confirmed the significantly effective prevention of necrotic spots on FC leaves caused by mancozeb. Additionally, FC leaves pre-treated with CFCFs showed a high reduction in the severity of leaf spots incited by the fungus Et, indicating the preventive effect of CFCFs against the pathogenic infection of the leaves. This effectiveness was most likely acquired because CFCFs could adhere to the leaf surface and remain on the inoculation sites, thus preventing the leaves from the later penetration of the fungus. Similarly, Yoshida et al. (2001) reported that pre-application of the CFCFs of *B. amyloliquefaciens* RC-2 suppressed anthracnose disease on mulberry leaves. In addition, we determined the suppressive effect of CFCFs on the leaf spots induced by the bacterium Bc, of which a 5-fold dilution of CFCFs resulted in the highest reduction of disease symptoms, similar to that of oxytetracycline applied at the recommended concentration. Hence, high concentrations of JCK-1618 and JCK-1696 CFCFs display great potential to replace synthetic chemicals in controlling leaf spots.

In this study, three CLPs, iturin A, fengycin A, and surfactin, were detected in the active fractions obtained from the culture filtrates of JCK-1618 and JCK-1696. Those compounds have also been identified from *B. amyloliquefaciens* JCK-12 (Kim et al., 2017) and *B. siamensis* JFL15 (Xu et al., 2018). Iturin and fengycin families exhibit high levels of antifungal properties against a wide range of fungal pathogens, and the vital roles of iturin A or fengycin in the suppression of fungal foliar diseases have been demonstrated (Li et al., 2016; Romero et al., 2007; Yoshida et al., 2001). In contrast, surfactin is limited for antifungal activity, but is shown to enhance the antifungal activity of other active CLPs when combined (Kim et al., 2017; Li et al., 2016) and as an antibacterial agent. Indeed, surfactin suppresses *P. syringae* infectivity in *Arabidopsis* (Bais et al., 2004). Taking this evidence into account, we conclude that iturin A, fengycin A, and surfactin were the main active compounds contributing to the antimicrobial activity of JCK-1618 and JCK-1696.

Difficidin and oxydifficidin, the oxidized form of difficidin, are reported as broad-spectrum antibacterial antibiotics, isolated from *B. subtilis* (Wilson et al., 1987) and *B. velezensis* (Im et al., 2020). The crucial role of difficidin purified from *B. velezensis* FZB42 in reducing the lesion lengths and disease severities in *X. oryzae* infections of rice leaves, has also been reported (Wu et al., 2015). Taken together with our findings, oxydifficidin, produced by JCK-1618 and JCK-1696, displayed crucial inhibitory effects on the growth of bacterial pathogens and the reduction of disease symptoms induced by the bacterium Bc.

Furthermore, both JCK-1618 and JCK-1696 secreted a variety of cell-wall degrading enzymes. Some of these have also been reported to be involved in antimicrobial activity against phytopathogenic fungi by breaking down cell-wall elements such as chitin, β-1,3-glucan, chitosan, and protein, and inhibiting fungal spore germination, including chitinases (Lorito et al., 1994; Mauch et al., 1988), β-1,3-glucanases (Lorito et al., 1994; Mauch et al., 1988), chitosanases (Gao et al., 2008) and proteases (Flores et al., 1997). The inhibitory action of purified chitinase against bacteria has been previously recorded (Wang and Chang, 1997). In the present study, crude enzymes obtained from JCK-1618 and JCK-1696 specifically hindered the growth of the fungi Et and Mc, which both contained chitin and β-1,3-glucan as the major components of their cell-walls, and three gram-negative bacteria, including Xap, Bc, and

Pss, thus indicating the possible roles of chitinases, β-1,3-glucanases, chitosanases, and proteases in antimicrobial activities.

In addition to acting as inhibitors against phytopathogenic microbes, JCK-1618 and JCK-1696 excreted IAA, a phytohormone previously detected in *Bacillus* species and known as an effector molecule in plant stimulation (Idris et al., 2007; Senthilkumar et al., 2009).

Biofilm formation is a widespread adaptive behavior of bacteria to survive in hostile environments and to disperse to colonize new niches (Hall-Stoodley et al., 2004). In addition to their involvement in bacterial motility, several *Bacillus* CLPs, such as fengycin (Cao et al., 2018), surfactin (Bais et al., 2004; Cao et al., 2018) and iturin A (Cao et al., 2018), have been reported to be crucially implicated in biofilm formation. Indeed, the two antagonists in the present study produced iturin A, fengycin A, and surfactin and were therefore able to form robust biofilms.

Collectively, the two *B. velezensis* strains, JCK-1618 and JCK-1696, inhibited the growth of the pathogens causing SH in FC trees through several antimicrobial agents, including diffusible CLPs and polyketides, hydrolytic enzymes, and VOCs. Additionally, the CFCFs of JCK-1618 and JCK-1696 significantly reduced leaf spot symptom severity in a detached leaf assay. The biochemical and phenotypic characteristics that may be involved in the antimicrobial activity and versatility of the two bacterial antagonists for the function of biocontrol have also been highlighted. To our knowledge, this is the first study focusing on the control of SH in FC trees, especially using antagonistic bacteria.

Conflicts of Interest

No potential conflict of interest relevant to this article was reported.

Acknowledgments

We thank Prof. In-Seon Kim (Pesticide Science Lab., Department of Agricultural Chemistry, Chonnam National University) for GC-MS technical assistance. This work was supported by a grant from the National Institute of Biological Resources (NIBR), funded by the Ministry of Environment (MOE) of South Korea (grant number: NIBR202018201).

Electronic Supplementary Material

Supplementary materials are available at The Plant Pathology Journal website (http://www.ppjonline.org/).

References

Bais, H. P., Fall, R. and Vivanco, J. M. 2004. Biocontrol of *Bacillus subtilis* against infection of Arabidopsis roots by *Pseudomonas syringae* is facilitated by biofilm formation and surfactin production. *Plant Physiol.* 134:307-319.

Bie, X., Lu, Z. and Lu, F. 2009. Identification of fengycin homologues from Bacillus subtilis with ESI-MS/CID. *J. Microbiol. Methods* 79:272-278.

Cao, Y., Pi, H., Chandrangsu, P., Li, Y., Wang, Y., Zhou, H., Xiong, H., Helmann, J. D. and Cai, Y. 2018. Antagonism of two plant-growth promoting *Bacillus velezensis* isolates against *Ralstonia solanacearum* and *Fusarium oxysporum*. *Sci. Rep.* 8:4360.

Chaves-López, C., Serio, A., Gianotti, A., Sacchetti, G., Ndagijimana, M., Ciccarone, C., Stellarini, A., Corsetti, A. and Paparella, A. 2015. Diversity of food-borne *Bacillus* volatile compounds and influence on fungal growth. *J. Appl. Microbiol.* 119:487-499.

Chen, X.-H., Koumoutsi, A., Scholz, R. and Borriss, R. 2009. More than anticipated - production of antibiotics and other secondary metabolites by *Bacillus amyloliquefaciens* FZB42. *J. Mol. Microbiol. Biotechnol.* 16:14-24.

Chun, J. and Bae, K.S. 2000. Phylogenetic analysis of *Bacillus subtilis* and related taxa based on partial gyrA gene sequences. *Antonie van Leeuwenhoek* 78:123-127.

Compant, S., Duffy, B., Nowak, J., Clément, C. and Barka, E. A. 2005. Use of plant growth-promoting bacteria for biocontrol of plant diseases: principles, mechanisms of action, and future prospects. *Appl. Environ. Microbiol.* 71:4951-4959.

De Souza, J. T., De Boer, M., De Waard, P., Van Beek, T. A. and Raaijmakers, J. M. 2003. Biochemical, genetic, and zoosporicidal properties of cyclic lipopeptide surfactants produced by *Pseudomonas fluorescens*. *Appl. Environ. Microbiol.* 69:7161-7172.

Díaz, R., Zas, R. and Fernández-López, J. 2007. Genetic variation of *Prunus avium* in susceptibility to cherry leaf spot (*Blumeriella jaapii*) in spatially heterogeneous infected seed orchards. *Ann. For. Sci.* 64:21-30.

Dunlap, C. A., Kim, S. J., Kwon, S. W. and Rooney, A. P. 2016. *Bacillus velezensis* is not a later heterotypic synonym of *Bacillus amyloliquefaciens; Bacillus methylotrophicus, Bacillus amyloliquefaciens* subsp. *plantarum* and '*Bacillus oryzicola*' are later heterotypic synonyms of *Bacillus velezensis* based on *phylogenomics*. *Int. J. Syst. Evol. Microbiol*. 66:1212-1217.

Elad, Y. and Baker, R. 1985. Influence of trace amounts of cations and siderophore-producing pseudomonads on chlamydospore germination of *Fusarium oxysporum*. *Phytopathology* 75:1047-1052.

Fan, B., Blom, J., Klenk, H.-P. and Borriss, R. 2017. *Bacillus amyloliquefaciens*, *Bacillus velezensis*, and *Bacillus siamen-*

sis form an "operational group *B. amyloliquefaciens*" within the *B. subtilis* species complex. *Front. Microbiol.* 8:22.

Faveri, M., Mayer, M. P. A., Feres, M., de Figueiredo, L. C., Dewhirst, F. E. and Paster, B. J. 2008. Microbiological diversity of generalized aggressive periodontitis by 16S rRNA clonal analysis. *Oral Microbiol. Immunol.* 23:112-118.

Fernando, W. G. D., Ramarathnam, R., Krishnamoorthy, A. S. and Savchuk, S. C. 2005. Identification and use of potential bacterial organic antifungal volatiles in biocontrol. *Soil Biol. Biochem.* 37:955-964.

Flores, A., Chet, I. and Herrera-Estrella, A. 1997. Improved biocontrol activity of *Trichoderma harzianum* by over-expression of the proteinase-encoding gene *prb1*. *Curr. Genet.* 31:30-37.

Gao, X.-A., Ju, W.-T., Jung, W.-J. and Park, R.-D. 2008. Purification and characterization of chitosanase from *Bacillus cereus* D-11. *Carbohydr. Polym.* 72:513-520.

Gordon, S. A. and Weber, R. P. 1951. Colorimetric estimation of indoleacetic acid. *Plant Physiol.* 26:192-195.

Gruber, B. R., Kruger, E. L. and McManus, P. S. 2012. Effects of cherry leaf spot on photosynthesis in tart cherry 'Montmorency' foliage. *Phytopathology* 102:656-661.

Gudiña, E. J., Rocha, V., Teixeira, J. A. and Rodrigues, L. R. 2010. Antimicrobial and antiadhesive properties of a biosurfactant isolated from *Lactobacillus paracasei* ssp. *paracasei* A20. *Lett. Appl. Microbiol.* 50:419-424.

Hall-Stoodley, L., Costerton, J. W. and Stoodley, P. 2004. Bacterial biofilms: from the natural environment to infectious diseases. *Nat. Rev. Microbiol.* 2:95-108.

Han, V.-C., Yu, N. H., Park A. E., Yoon, H., Son, Y. K., Lee, B.-H. and Kim, J.-C. 2021a. First report of shot-hole on flowering cherry caused by *Burkholderia contaminans* and *Pseudomonas syringae* pv. *syringae*. *Plant Dis.* 105:3795-3802.

Han, V.-C., Yu, N. H., Yoon, H., Son, Y. K., Lee, B.-H. and Kim, J.-C. 2021b. First report of *Epicoccum tobaicum* associated with leaf spot on flowering cherry in South Korea. *Plant Dis.* 105:2734.

Hulin, M. T., Mansfield, J. W., Brain, P., Xu, X., Jackson, R. W. and Harrison, R. J. 2018. Characterization of the pathogenicity of strains of *Pseudomonas syringae* towards cherry and plum. *Plant Pathol.* 67:1177-1193.

Idris, E. E., Iglesias, D. J., Talon, M. and Borriss, R. 2007. Tryptophan-dependent production of indole-3-acetic acid (IAA) affects level of plant growth promotion by *Bacillus amyloliquefaciens* FZB42. *Mol. Plant-Microbe Interact.* 20:619-626.

Im, S. M., Yu, N. H., Joen, H. W., Kim, S. O., Park, H. W., Park, A. R. and Kim, J.-C. 2020. Biological control of tomato bacterial wilt by oxydifficidin and difficidin-producing *Bacillus methylotrophicus* DR-08. *Pestic. Biochem. Physiol.* 163:130-137.

Kim, K., Lee, Y., Ha, A., Kim, J.-I., Park, A. R., Yu, N. H., Son, H., Choi, G. J., Park, H. W., Lee, C. W., Lee, T., Lee, Y.-W. and Kim, J.-C. 2017. Chemosensitization of *Fusarium graminearum* to chemical fungicides using cyclic lipopeptides produced by *Bacillus amyloliquefaciens* strain JCK-12. *Front. Plant Sci.* 8:2010.

Kruijt, M., Tran, H. and Raaijmakers, J. M. 2009. Functional, genetic and chemical characterization of biosurfactants produced by plant growth-promoting *Pseudomonas putida* 267. *J. Appl. Microbiol.* 107:546-556.

Kumar, S., Stecher, G., Li, M., Knyaz, C. and Tamura, K. 2018. MEGA X: molecular evolutionary genetics analysis across computing platforms. *Mol. Biol. Evol.* 35:1547-1549.

Lee, J. P., Lee, S.-W., Kim, C. S., Son, J. H., Song, J. H., Lee, K. Y., Kim, H. J., Jung, S. J. and Moon, B. J. 2006. Evaluation of formulations of Bacillus licheniformis for the biological control of tomato gray mold caused by *Botrytis cinerea*. *Biol. Control* 37:329-337.

Li, Q., Ning, P., Zheng, L., Huang, J., Li, G. and Hsiang, T. 2010. Fumigant activity of volatiles of *Streptomyces globisporus* JK-1 against *Penicillium italicum* on *Citrus microcarpa*. *Postharvest Biol. Technol.* 58:157-165.

Li, X., Zhang, Y., Wei, Z., Guan, Z., Cai, Y. and Liao, X. 2016. Antifungal activity of isolated *Bacillus amyloliquefaciens* SYBC H47 for the biocontrol of peach gummosis. *PLoS ONE* 11:e0162125.

López-Lara, I. M., Nogales, J., Pech-Canul, Á., Calatrava-Morales, N., Bernabéu-Roda, L. M., Durán, P., Cuéllar, V., Olivares, J., Alvarez, L., Palenzuela-Bretones, D., Romero, M., Heeb, S., Cámara, M., Geiger, O. and Soto, M. J. 2018. 2-Tridecanone impacts surface-associated bacterial behaviours and hinders plant-bacteria interactions. *Environ. Microbiol.* 20:2049-2065.

Lorito, M., Peterbauer, C., Hayes, C. K. and Harman, G. E. 1994. Synergistic interaction between fungal cell wall degrading enzymes and different antifungal compounds enhances inhibition of spore germination. *Microbiology* 140:623-629.

Mauch, F., Mauch-Mani, B. and Boller, T. 1988. Antifungal hydrolases in pea tissue: II. Inhibition of fungal growth by combinations of chitinase and β-1,3-glucanase. *Plant Physiol.* 88:936-942.

Morita, T., Tanaka, I., Ryuda, N., Ikari, M., Ueno, D. and Someya, T. 2019. Antifungal spectrum characterization and identification of strong volatile organic compounds produced by *Bacillus pumilus* TM-R. *Heliyon* 5:e01817.

Nautiyal, C. S. 1999. An efficient microbiological growth medium for screening phosphate solubilizing microorganisms. *FEMS Microbiol. Lett.* 170:265-270.

Nguyen, H. T., Kim, S., Yu, N. H., Park, A. R., Yoon, H., Bae, C.-H., Yeo, J. H., Kim, I. S. and Kim, J.-C. 2019. Antimicrobial activities of an oxygenated cyclohexanone derivative isolated from *Amphirosellinia nigrospora* JS-1675 against various plant pathogenic bacteria and fungi. *J. Appl. Microbiol.* 126:894-904.

O'Toole, G. A., Pratt, L. A., Watnick, P. I., Newman, D. K., Weaver, V. B. and Kolter, R. 1999. Genetic approaches to study of biofilms. *Methods Enzymol.* 310:91-109.

Proffer, T. J., Lizotte, E., Rothwell, N. L. and Sundin, G. W. 2013. Evaluation of dodine, fluopyram and penthiopyrad for the

management of leaf spot and powdery mildew of tart cherry, and fungicide sensitivity screening of Michigan populations of *Blumeriella jaapii*. *Pest Manag. Sci.* 69:747-754.

R Core Team. 2018. R: a language and environment for statistical computing. URL https://www.r-project.org/ [14 Febuary 2022].

Raza, W., Ling, N., Yang, L., Huang, Q. and Shen, Q. 2016. Response of tomato wilt pathogen *Ralstonia solanacearum* to the volatile organic compounds produced by a biocontrol strain *Bacillus amyloliquefaciens* SQR-9. *Sci. Rep.* 6:24856.

Romero, D., de Vicente, A., Rakotoaly, R. H., Dufour, S. E., Veening, J.-W., Arrebola, E., Cazorla, F. M., Kuipers, O. P., Paquot, M. and Pérez-García, A. 2007. The iturin and fengycin families of lipopeptides are key factors in antagonism of *Bacillus subtilis* toward *Podosphaera fusca*. *Mol. Plant-Microbe Interact*. 20:430-440.

Schallmey, M., Singh, A. and Ward, O. P. 2004. Developments in the use of *Bacillus* species for industrial production. *Can. J. Microbiol.* 50:1-17.

Schwyn, B. and Neilands, J. 1987. Universal chemical assay for the detection and determination of siderophores. *Anal. Biochem.* 160:47-56.

Senthilkumar, M., Swarnalakshmi, K., Govindasamy, V., Lee, Y. K. and Annapurna, K. 2009. Biocontrol potential of soybean bacterial endophytes against charcoal rot fungus, *Rhizoctonia bataticola. Curr. Microbiol.* 58:288-293.

Shemesh, M. and Chai, Y. 2013. A combination of glycerol and manganese promotes biofilm formation in *Bacillus subtilis* via histidine kinase KinD signaling. *J. Bacteriol.* 195:2747-2754.

Tahir, H. A. S., Gu, Q., Wu, H., Niu, Y., Huo, R. and Gao, X. 2017. *Bacillus* volatiles adversely affect the physiology and ultra-structure of *Ralstonia solanacearum* and induce systemic resistance in tobacco against bacterial wilt. *Sci. Rep.* 7:40481.

Wang, S. L. and Chang, W.-T. 1997. Purification and characterization of two bifunctional chitinases/lysozymes extracellularly produced by *Pseudomonas aeruginosa* K-187 in a shrimp and crab shell powder medium. *Appl. Environ. Microbiol.* 63:380-386.

Williams-Woodward, J. L. 1998. Effect of fungicide treatment to control shot-hole disease of cherry laurel. URL http://www.canr.org/98013.pdf [14 Febuary 2022].

Wilson, K. E., Flor, J. E., Schwartz, R. E., Joshua, H., Smith, J. L., Pelak, B. A., Liesch, J. M. and Hensens, O. D. 1987. Difficidin and oxydifficidin: novel broad spectrum antibacterial antibiotics produced by *Bacillus subtilis*. II. Isolation and physico-chemical characterization. *J. Antibiot.* 40:1682-1691.

Wu, L., Wu, H., Chen, L., Yu, X., Borriss, R. and Gao, X. 2015. Difficidin and bacilysin from Bacillus amyloliquefaciens FZB42 have antibacterial activity against *Xanthomonas oryzae* rice pathogens. *Sci. Rep.* 5:12975.

Xu, B.-H., Lu, Y.-Q., Ye, Z.-W., Zheng, Q.-W., Wei, T., Lin, J.-F. and Guo, L.-Q. 2018. Genomics-guided discovery and structure identification of cyclic lipopeptides from the *Bacillus siamensis* JFL15. *PLoS ONE* 13:e0202893.

Xu, S. J. and Kim, B. S. 2014. Biocontrol of fusarium crown and root rot and promotion of growth of tomato by *Paenibacillus* strains isolated from soil. *Mycobiology* 42:158-166.

Yoshida, S., Hiradate, S., Tsukamoto, T., Hatakeda, K. and Shirata, A. 2001. Antimicrobial activity of culture filtrate of *Bacillus amyloliquefaciens* RC-2 isolated from mulberry leaves. *Phytopathology* 91:181-187.

Yuan, J., Raza, W., Shen, Q. and Huang, Q. 2012. Antifungal activity of *Bacillus amyloliquefaciens* NJN-6 volatile compounds against *Fusarium oxysporum* f. sp. *cubense*. *Appl. Environ. Microbiol.* 78:5942-5944.

Zhang, X., Li, B., Wang, Y., Guo, Q., Lu, X., Li, S. and Ma, P. 2013. Lipopeptides, a novel protein, and volatile compounds contribute to the antifungal activity of the biocontrol agent *Bacillus atrophaeus* CAB-1. *Appl. Microbiol. Biotechnol.* 97:9525-9534.

Zheng, M., Shi, J., Shi, J., Wang, Q. and Li, Y. 2013. Antimicrobial effects of volatiles produced by two antagonistic *Bacillus* strains on the anthracnose pathogen in postharvest mangos. *Biol. Control* 65:200-206.

Zlatković, M., Keča, N., Wingfield, M. J., Jami, F. and Slippers, B. 2016. Shot hole disease on *Prunus laurocerasus* caused by *Neofusicoccum parvum* in Serbia. *For. Pathol.* 46:666-669.